Recursive Actuator Fault Detection and Diagnosis for Emergency Landing of UASs

X. Yang * L. Mejias * M. Warren * F. Gonzalez * B. Upcroft **

* Australian Research Center for Aerospace Automation (ARCAA) and
Queensland University of Technology (QUT), Brisbane, Australia.
(e-mail: {xilin.yang, luis.mejias, michael.warren,
felipe.gonzalez}@qut.edu.au).
** School of EECS, QUT, Brisbane, Australia.(e-mail:
ben.upcroft@qut.edu.au)

Abstract: This paper presents a practical recursive fault detection and diagnosis (FDD) scheme for online identification of actuator faults for unmanned aerial systems (UASs) based on the unscented Kalman filtering (UKF) method. The proposed FDD algorithm aims to monitor health status of actuators and provide indication of actuator faults with reliability, offering necessary information for the design of fault-tolerant flight control systems to compensate for side-effects and improve fail-safe capability when actuator faults occur. The fault detection is conducted by designing separate UKFs to detect aileron and elevator faults using a nonlinear six degree-of-freedom (DOF) UAS model. The fault diagnosis is achieved by isolating true faults by using the Bayesian Classifier (BC) method together with a decision criterion to avoid false alarms. High-fidelity simulations with and without measurement noise are conducted with practical constraints considered for typical actuator fault scenarios, and the proposed FDD exhibits consistent effectiveness in identifying occurrence of actuator faults, verifying its suitability for integration into the design of fault-tolerant flight control systems for emergency landing of UASs.

Keywords: Fault diagnosis and isolation; unscented Kalman filter; multiple-model adaptive estimation; emergency landing; unmanned aerial system.

1. INTRODUCTION

UASs have proved effective in a number of civilian operations such as power line inspection, bush fire investigation and urban traffic monitoring. They also have great potential to reduce cost and requirements for life support due to recent development in UAS technology (Kendoul (2013); Bernard et al. (2011)). However, one of the key issues which remains unresolved is the demand for an emergency landing system in case of accidental actuator faults, especially when UASs are operating over populated areas. In such situations, UASs are expected to be equipped with sufficient capability to identify suitable landing sites and accommodate faults to achieve safe emergency landing. This requires automated implementation of several systems onboard the UAS. A landing site decision method is required which aims to provide feasible landing locations given information about land texture, surface flatness and turning rate constraints. A fault-tolerant flight control system is also necessary which can detect, isolate and accommodate online actuator faults.

Emergency landing of UASs has received increasing attention in the past decades due to occurrence of accidental crash caused by mechanical failures (engine, actuator, etc.) or loss of stability in extreme weather conditions (strong gusts, storm, etc.). Several important aspects of emergency landing has been investigated in the literature.

Development of a fault-tolerant guidance, navigation and control system to improve emergency landing reliability and minimize threat to the community has been addressed in a number of references (Ducard (2009); Zhang and Jiang (2000); Calise et al. (2001); Brinker and Wise (2001)). Ducard (2009) designed a fault-tolerant control system which focuses on the FDD of faults among sensors and actuators and on development of a reconfigurable control allocation module. A fault-tolerant control system was proposed by Zhang and Jiang (2000) which possesses the ability to accommodate system component failures. This system comprises a FDD scheme, a reconfigurable controller and a control reconfiguration mechanism. Also, Identification of appropriate landing sites for trajectory planning in emergency situations has been addressed by some researchers (Williams and Crump (2012); Mejias et al. (2009); Mejias and Fitzgerald (2013)). Mejias et al. (2009) proposed a computer vision based procedure to identify emergency landing sites based on size, shape, slope and texture of surfaces to achieve automatic classification of the candidate landing sites. Williams and Crump (2012) provided flight-test results of a landing system which utilizes prior location information to decide the most feasible landing sites.

Onboard fault detection and diagnosis has also been investigated in the literature for several aerospace applications. The multiple-model adaptive estimation (MMAE) scheme

has proven to be effective and been applied to dealing with FDD problems in various flight scenarios (Maybeck (1999); Eide and Maybeck (1996); Meskin et al. (2013); Amirarfaei et al. (2013)). A bank of parallel Kalman filters was adopted with each matched to a specific hypothesis on the failure status by Maybeck (1999). The authors also developed a hierarchical structure to keep the number of online filters to a minimum. However, linear Kalman filters only function effectively around operating conditions, and a series of linearized flight models are required for the FDD purpose to cover the whole flight envelope. This would greatly aggravate onboard computational burden. Further, this algorithm would collapse in situations where linearized models do not exist. The MMAE with extended Kalman filters (EKF) incorporated has been proposed for fault estimation in Ducard (2009); Ducard and Geering (2008). The validity of EKFs is based on the existence of Jacobian matrices of the system model under all possible flight conditions. Moreover, in situations where system dynamics change abruptly, Jacobian matrices might not exist or have singular issues (Julier and Uhlmann (2004)), and EKF-based MMAE would fail to detect occurrence of faults. Therefore, in our case where flight dynamics are subject to abrupt changes when accidental faults occur, we will develop a UKF-based FDD procedure. Campbell and Brunke (2001) demonstrate that the UKFs show performance improvement when compared with the EKFs for a nonlinear F-16 like aircraft model. Another possible solution to the online FDD is the interactive multiple model (IMM) method. The IMM employs parallel filters which interact with each other for performance improvement at the expense of high computational and storage requirements (Zhang and Li (1998); Kim et al. (2008); Lee et al. (2005)). This is due to the fact that the initial estimate at the beginning of each cycle is a mixture of all most recent estimates (Zhang and Li (1998)). In our work, we are aimed at a feasible estimation approach which can be implemented at the cost of limited flight computer memory and provide sufficient estimation accuracy. Thus, we use the MMAE with UKFs to perform the FDD of actuator faults.

The current research is part of the ResQu project which aims to develop automated safety technologies for UAS safe recovery by providing a feasible emergency landing system with autonomous vision-based site decision and robust navigation, guidance and control capabilities. In this research, we aim to develop an online FDD procedure to monitor occurrence of actuator faults with minimum time delay, and conduct fault detection when a UAS operates in a wide range of flight envelopes. The proposed algorithm should also consider computational burden and FDD reliability. To this end, a nonlinear 6-DOF dynamic model in consideration of aerodynamic forces and moments is explored. The UKF algorithm is designed based on the nonlinear model and excludes the need for calculating the Jacobian matrices. The aileron and elevator are treated as additional system states in the augmented state vector, and are estimated by the UKF algorithm. To avoid false alarms of faulty actuators, a recursive fault diagnosis algorithm is designed based on the measurement residuals and error covariance of the UKF. Performance of the FDD is evaluated using a high-fidelity 6-DOF UAS model. Simulations are conducted to verify performance

of the proposed FDD scheme, and it is demonstrated that actuator faults can be identified with guarantees.

2. FLIGHT DYNAMICS OF A UAS

In practice, emergency landing is required as a result of occurrence of possible actuator faults under various flight scenarios (steady-state, bank-to-burn, skid-to-turn, etc). In the considered application which requires a detection and diagnosis procedure to cover entire flight regions, the nonlinear 6-DOF dynamic model is developed in consideration of aerodynamic and propulsive forces and moments. Details of the nonlinear dynamics are given in Yang et al. (2013). We are concerned with a UAS model with variable flight speeds as faults might occur during any phase of flight. Thus, the current model is different from the one which assumes constant flight speeds in Yang et al. (2013).

The continuous-time system model is discretized using the Euler integral method, and can be described by

$$x(k + 1) = f(x(k), u(k)) + \epsilon(k) \qquad (1)$$

where state vector x refers to 8 state variables

$$x = [u, v, w, p, q, r, \phi, \theta]^T \qquad (2)$$

and actuator inputs are $u = [\delta_a, \delta_e]^T$. Process noise $\epsilon = [\epsilon_1, \cdots, \epsilon_8]^T$ is mutually independent Gaussian distributions and satisfies

$$E[\epsilon(k)] = 0, \; E[\epsilon(k)\epsilon^T(i)] = \delta(k - i)Q(k) \qquad (3)$$

where $\delta(\cdot)$ is the Kronecker function and $Q(k)$ is process error covariance.

The measurement equation is

$$y(k) = C \cdot x(k) + \xi(k) \qquad (4)$$

The constant matrix $C = I_{8 \times 8}$ and measurement noise with Gaussian distribution $\xi = [\xi_1, ..., \xi_8]^T$ satisfies

$$E[\xi(k)] = 0, \; E[\xi(k)\xi^T(i)] = \delta(k - i)R(k) \qquad (5)$$

where $R(k)$ is the measurement noise covariance.

3. UKF-BASED FAULT DETECTION

The MMAE is an effective approach to online detection of system faults/failures. This method relies on a bank of Kalman filters with each matching a particular system mode (faulty or non-faulty). In our case, we are aimed at developing a UKF-based MMAE scheme to cover a wide range of flight conditions with reasonable computational efficiency. Given this requirement, it is desired that a complete set of system modes are to be explored, and each is associated with evident separation properties. Measurement residuals are a key factor to determine proper system modes and distinct differences in them make the modes identifiable by the UKF models. Furthermore, fault isolation is achieved by computing model probabilities which also rely on measurement residuals. Therefore, we will build UKF models with each accompanied with notable separation properties.

In our case, there are three possible modes: non-fault, aileron fault and elevator fault. Thus, the filter design process is formulated as the construction of filter models

to represent dynamics of possible system behaviors by employing the following N pairs of equations:

$$x_i(k+1) = f_i(x_i(k), u_i(k)) + \epsilon_i(k) \tag{6}$$
$$y_i(k) = C_i(k)x_i(k) + \xi_i(k) \tag{7}$$

Here, subscript $i \in N$ relates to the mode $m_i \in Z$. The model set $Z = \{m_0, m_a, m_e\}$ contains $N(N = 3)$ possible system modes where m_0 refers to the non-fault mode, m_a the aileron fault and m_e the elevator fault. Also, $f_i(\cdot)$ and $C_i(\cdot)$ are of different structures for different system modes.

There are several recursive filter options available (EKF and UKF, etc.) for nonlinear systems. The UKF-based filters are preferred as singular issues can be avoided. In the considered application, three single-filter-based UKFs are developed with the first one for non-fault mode and the other two for actuator faults. The two UKFs for actuator fault detection are derived with each monitoring the health status of one actuator. System model (Eq. (1)) and measurement model (Eq. (4)) can only be used for state estimate in the non-fault scenario, and an augmented system model is required with adequate modifications to detect a specific actuator fault. We follow the strategy in Ducard (2009) and augment the state vector as

$$x_j = [x_i^T, \delta_j]^T \tag{8}$$

where $\delta_j, j = a, e$ refers to the aileron or elevator. This definition considers the monitored actuator as an additional state variable. Thus, control action from the δ_j to flight performance is neglected and the status of the δ_j actuator is estimated through conducting the UKF procedure.

The fault detection is conducted by designing separate UKFs for ailerons and elevators, as shown in Fig. 1. Inputs to each UKF are measured system states and other available information (angle-of-attack, sideslip, thrust, etc.). The UKF algorithm is able to detect actuator faults without knowledge of health status of any actuator. When detecting aileron fault, the estimated elevator signal from UKF2 is considered as a replica of the actual elevator command. Thus, UKF1 is able to estimate status of aileron. Similarly, UKF2 takes estimated aileron command from UKF1 as actual aileron and outputs estimate of elevator status. Thus, the detection algorithm can be considered as a black-box which takes measured states as inputs and outputs status of actuators.

4. RECURSIVE FAULT DIAGNOSIS

4.1 Calculation of Fault Probability

Fault diagnosis refers to isolation of true faults which can be used to trigger fault-tolerant control strategies. Occasionally, actuator faults occur instantly and disappear rapidly. These expeditious faults are often of low magnitude and cause ignorable effect on the handling quality of a UAS due to the short duration. Thus, flight stability can still be maintained by existing proportional-integral-derivative (PID) controllers. However, in the event of true actuator faults characterized by an evident time duration and significant magnitude, it is required that these faults are identified with maximum probability such that confident fault isolation is achieved which can trigger the emergency landing procedure timely.

In the MMAE framework, each UKF generates an estimate of the system states, and the actual system states are the summation of these state vectors weighted by the corresponding conditional probability (Maybeck (1999)),

$$\hat{x}(k) = \sum_{i=1}^{N} P_i(k)x_i(k) \tag{9}$$

Here, the index i covers all possible faulty modes including the non-fault mode. The probability $P_i(k)$ is the posterior conditional probability that declares the faulty mode $m = m_i$ given the observed measurements up to the time instant k,

$$P_i(k) = Pr[m = m_i|Y_k], \quad Y_k = \{y_0, \cdots, y_k\} \tag{10}$$

where measurement history vector Y_k contains available measurements at different time instants $t_0, \cdots, t_k$.

For online fault isolation, $P_i(k)$ can be computed by the recursive Bayesian Classifier (BC) (Ducard (2009); Maybeck (1999))

$$P_i(k) = \frac{P[y = y_k|m = m_i, Y_{k-1}]P_i(k-1)}{\sum_{j=0}^{N} P[y = y_k|m = m_j, Y_{k-1}]P_j(k-1)} \tag{11}$$

with the conditional probability density for the current measurement y_k given by

$$P[y = y_k|m = m_i, Y_{k-1}] = \alpha_i(k)e^{-S_i(k)} \tag{12}$$

where

$$\alpha_i(k) = (2\pi)^{-\frac{m}{2}} |\Sigma_i(k)|^{-\frac{1}{2}} \tag{13}$$

$$S_i(k) = \frac{r_i^T(k)\Sigma_i^{-1}(k)r_i(k)}{2} \tag{14}$$

Here, i is actuator fault mode, N is number of actuator faults. Residual is $r_i(k) = y_i(k) - \mu_i(k)$ where $y_i(k)$ is measurement vector and $\mu_i(k)$ predicted mean of measurement from the UKF. Therefore, the complete recursive form to compute fault probabilities at time instant k is

$$P_i(k) = \frac{\alpha_i(k)e^{-S_i(k)} \cdot P_i(k-1)}{\sum_{j=0}^{N} \alpha_j(k)e^{-S_j(k)} \cdot P_j(k-1)} \tag{15}$$

where $j \in \{0, a, e\}$ indicates an actuator fault. In practice, it is found that the leading term $\alpha_i(k)$ can be neglected in the recursive process (Eide and Maybeck (1996)).

In our case, the BC approach conducts hypothesis testing by assuming Gaussian distributions of the measurement residuals. This method functions effectively when system dynamics are contaminated by noise with Gaussian distributions. Essentially, the UKF corresponding to the true fault scenario would generate an estimated measurement vector most close to the the observed measurement vector, and yield the minimum residuals which result in the largest probability to indicate the proper UKF in consonance with the true fault scenario.

Remark 1. To avoid false alarms, the detected fault is claimed to be true when the corresponding fault probability exceeds 0.95 for ten consecutive sampling points.

Remark 2. As we are concerned with emergency situations where actuator faults occur abruptly, the UAS is assumed steady-state flight conditions at the initial stage. Thus, the initial probability for non-fault case is set to be unity and probabilities for faulty actuators are set to be zero. The probability will converge to declare the fault mode once actuator fault occurs.
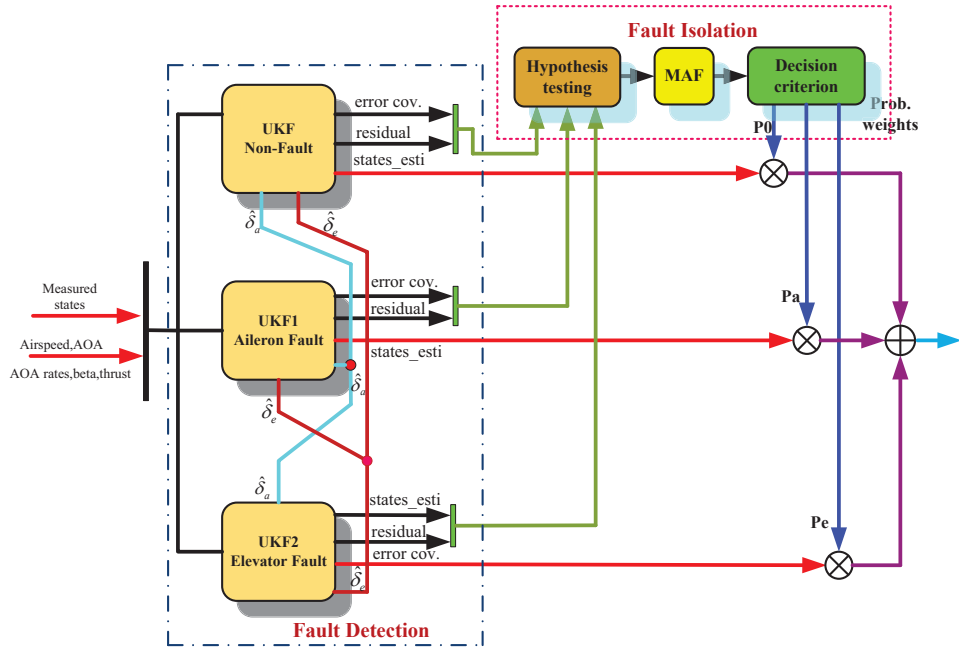
Fig. 1. UKF-based fault detection and diagnosis scheme

Remark 3. In the recursion process, low bounds for the probabilities are set to be 0.001 to prevent locking into zero which would prevent the recursion algorithm from converging to true probabilities.

4.2 Design of moving average filters

The probabilities generated from the BC are subject to short-term fluctuations which obscure probability trend. A proper filter is required to highlight the long-term trend of probability without causing significant time delay for fault identification. Three moving average filters (MAFs) are designed to smooth out the raw probabilities from the BC with proper window widths. These filters cannot be initiated efficiently until sufficient raw probability samples are collected and stored in the computer memory. In our case, a window width of 20 points was chosen after a few trails.

4.3 Actuator Fault Isolation

Even though the filtered probabilities become less noisy and performance of fault isolation has been improved, the isolation performance is yet to be satisfactory. For some time instant, it is observed that the true fault probability is ambiguous and not notably dominant over other probabilities. This causes difficulties in distinguishing true actuator faults and would result in false alarms. Ducard (2009) imposed an supervision module to monitor probability signals which assists in confirmation of actuator faults by adding excitation signals. There was also an additional filtering stage with lower and upper bounds to isolate true faults. These bounds are chosen empirically to extract dominant probabilities.

In our case, we employ a decision criterion proposed by Zhang and Li (1998):

$$P_j(k) = \max_{m_i \in Z} P_i(k), i = \{0, a, e\} \tag{16}$$

where Z refers to actuator fault model space $Z = \{m_0, m_a, m_e\}$.

$$P_H(k) = \frac{P_j(k)}{\max_{i \neq j, m_i \in Z} P_i(k)} \tag{17}$$

$$\text{if } P_H(k) \geq P_T \Rightarrow H_j : \text{Fault } j \text{ occurs,} \tag{18}$$

$$\text{if } P_H(k) < P_T \Rightarrow H_0 : \text{No fault occurs} \tag{19}$$

where P_T is the probability threshold. This decision logic is based on determination of a single threshold and facilitates the implementation in practice. The choice of threshold P_T is problem-dependent, and different values are used for different systems. Practically, the threshold begins with an empirical value and is determined after a few trials. The proper threshold is selected to reduce isolation time delay and avoid missing detection.

The block diagram of the proposed FDD is illustrated in Fig. 1. Based on the available measurements, the fault detection part constructs three UKFs which each monitoring a particular type of fault (including the non-fault scenario). The residuals and error covariance of each UKF are input into the hypothesis testing block to generate raw probabilities, which are then filtered by the MAFs to highlight long-term trends. The true probability weights for each mode are obtained after the filtered probabilities are regulated by the decision criterion. The estimated system states are the probabilistically weighted sum of the states from each UKF.

5. SIMULATION RESULTS

In this section, we test performance of the proposed FDD procedure for typical actuator faults which are likely to occur during flight. To identify and remedy possible deficiencies of the procedure before real-time implementation, we set up a high-fidelity simulation model based on parameters of one of ARCAA UASs by using the *AeroSim* simulation blockset. The AeroSim library provides a complete
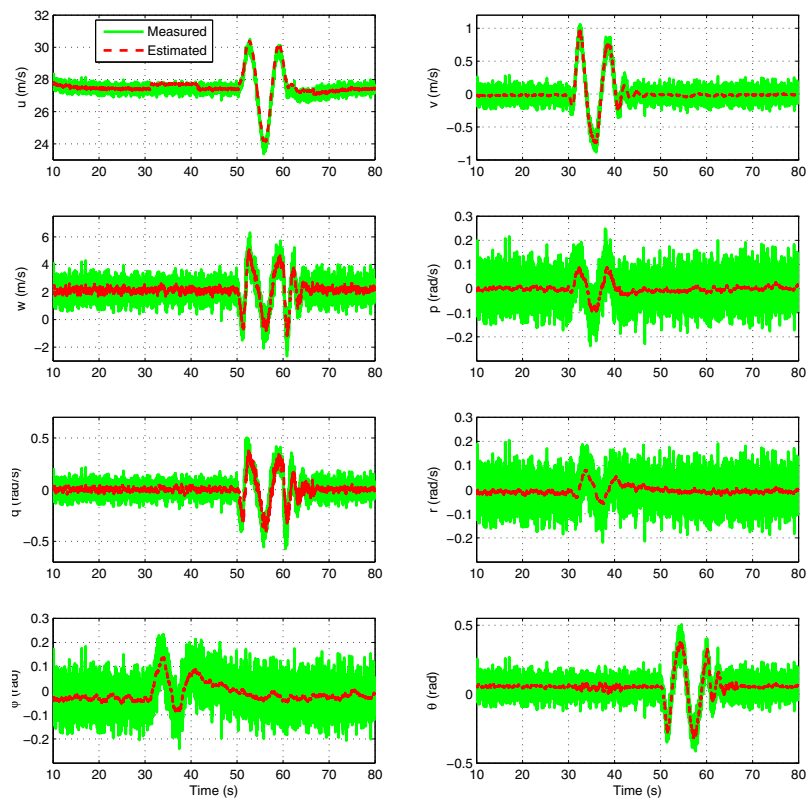
Fig. 4. Estimated states for floating faults
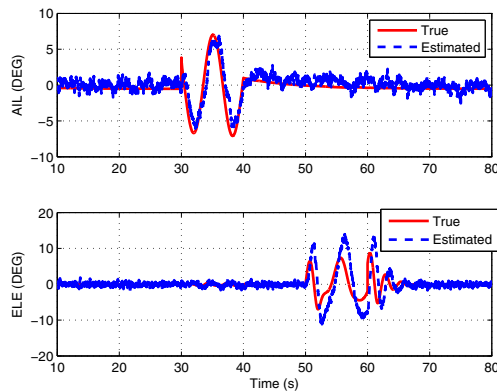
Fig. 2. Comparison of true and estimated actuator command for single floating faults

Fig. 3. Probabilities generated by the fault isolation decision criterion for single floating faults

set of tools for developing nonlinear aircraft models for overall evaluation of the FDD. Aerodynamic parameters of our UAS platform can be found in Yang et al. (2013).

In simulations, our UAS is controlled to be within the operational velocity range of $[20.83m/s, 57.78m/s]$. Also, operational limits on elevators and ailerons are imposed ($\delta_e \in [-25^o, 25^o]$ and $\delta_a \in [-15^o, 15^o]$). The angle of attack and sideslip are stabilized to change within the scope of $-5^o \leq \alpha \leq 5^o$ and $-28^o \leq \beta \leq 28^o$. Moreover, measurement noise in velocities, attitudes and angular

rates are considered with progressive increasing levels to test the performance of the FDD procedure. Two PID controllers are designed for aileron and elevator to achieve steady-state flight conditions. A group of control gains are selected to satisfy performance specifications such as settling time ($< 100s$) and steady-state errors ($< \%5$). Empirically, the proper control gains were found after a few trails with $k_{ap} = 0.2279, k_{ai} = 0.0027$ and $k_{ad} =$

0.2 for the aileron control, and $k_{ep} = -0.055, k_{ei} = -0.01$ and $k_{ed} = -0.1$ for the elevator control.

5.1 Detection and Diagnosis of Single Actuator Faults

Performance evaluation for single faults is firstly conducted for sequential occurrence of actuator faults. There are two typical actuator faults: floating fault and lock-in-place (LIP) fault. The floating fault describes a fluctuating actuator surface moving up and down without staying at a desired position. The LIP fault refers to the situation where the actuator is stuck at an unexpected location. In simulations, both faults occur and last for a certain period of time. Numerous simulations have been carried out and performance for single floating fault scenarios is illustrated in Fig. 2 and Fig. 3. As we are only concerned with faults during steady-state flight, the transient response in the first $10s$ is removed for observation convenience. Two separate floating faults are generated with an aileron fault occurring at time interval $[30s, 40s]$ and an elevator fault at $[50s, 65s]$. It is observed that the aileron fault is consistently estimated when floating fault occurs within $[-7^o, 7^o]$. In the time interval where elevator fault occurs within $[-8^o, 8^o]$, the UKF is able to detect the fault with rapid response. The estimate time delay is approximately $0.4s$ for aileron fault and $0.5s$ for the elevator fault. This is considered to be sufficient to conduct fault isolation onboard to distinguish true faults.

The fault isolation performance is shown in Fig. 3. It is seen that the raw probabilities from the BC are sensitive and will lead to false alarms. In the initial stage, probabilities for both aileron and elevator are zero. When the probabilities for aileron increase abruptly (shown as spikes in Fig. 3), these probabilities are set to zero after the filtering stage to avoid false alarms as they are less than 0.95 or last for less than 10 consecutive points. Only probabilities larger than 0.95 with a duration of 10 successive points are treated true faults. The decision threshold is chosen to be $P_T = 14$ after a few trials for fault isolation purpose. It is noticed that the actual aileron and elevator faults are effectively detected and isolated with rapid response. The estimated system states calculated from Eq. (9) are illustrated in Fig. 4. They are probabilistically weighted sum of the estimated states from different UKFs. It is observed that the proposed FDD is able to consistently estimate local velocities, angular rates and attitudes with a sufficient accuracy from the noisy measurements. When the estimated system states deviate from the steady-state values, our FDD procedure can detect and isolate true faults within a short period of time.

Performance of the FDD method is also tested for LIP actuator faults. Two individual LIP faults are created for aileron and elevator as shown in Fig. 5. It is observed that when LIP faults occur, it takes longer time to recover to the nominal values. Further, the coupling effect has the potential to result in an elevator fault when the aileron fault occurs. It is found that our procedure is able to detect and isolate an aileron fault within $[-5^o, 5^o]$. It is shown in Fig. 5 that single LIP fault in aileron is accurately detected and isolated with a time delay of $0.4s$. For a continuous LIP fault, it is seen that the estimate error increases due to the fact that it takes time for the UKFs to track the
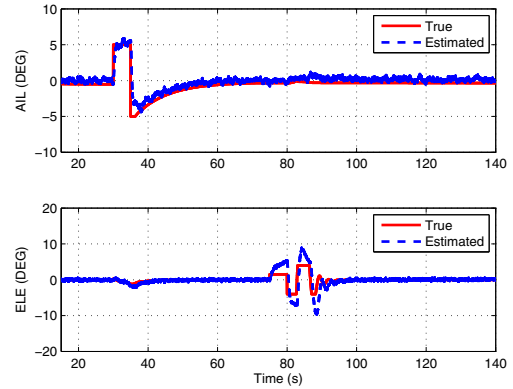
Fig. 5. Comparison of true and estimated actuator command for single LIP faults
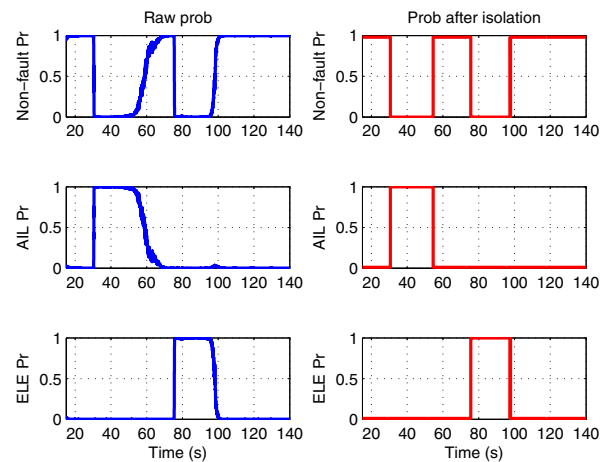
Fig. 6. Probabilities generated by the fault isolation decision criterion for LIP faults

system dynamics. Thus, this leads to transient responses. However, the LIP fault is still identified with a short time delay as can be seen in Fig. 6. It is shown in Fig. 7 that the estimated system states are accurately estimated from noisy measurements and can be used to evaluate flight conditions of a UAS.

5.2 Performance Evaluation for Measurement Noise

Measurement noise is an inevitable factor affecting estimate performance in real-time applications. The sensitivity analysis of our FDD method indicates that detection and isolation performance would degrade with an increase in measurement noise levels. To assess the tolerable limit for the proposed FDD, Gaussian random noise is imposed with progressively increasing levels in simulations. The following quantitative specifications are employed to evaluate the estimate performance:

$$\sigma = \sqrt{\frac{1}{N}\sum_{k=1}^{N}(x(k) - \bar{x}(k))^2} \qquad (20)$$

The estimate capacity factor γ is

$$\gamma = 20\log_{10}\frac{\sigma}{x_{max}} \qquad (21)$$
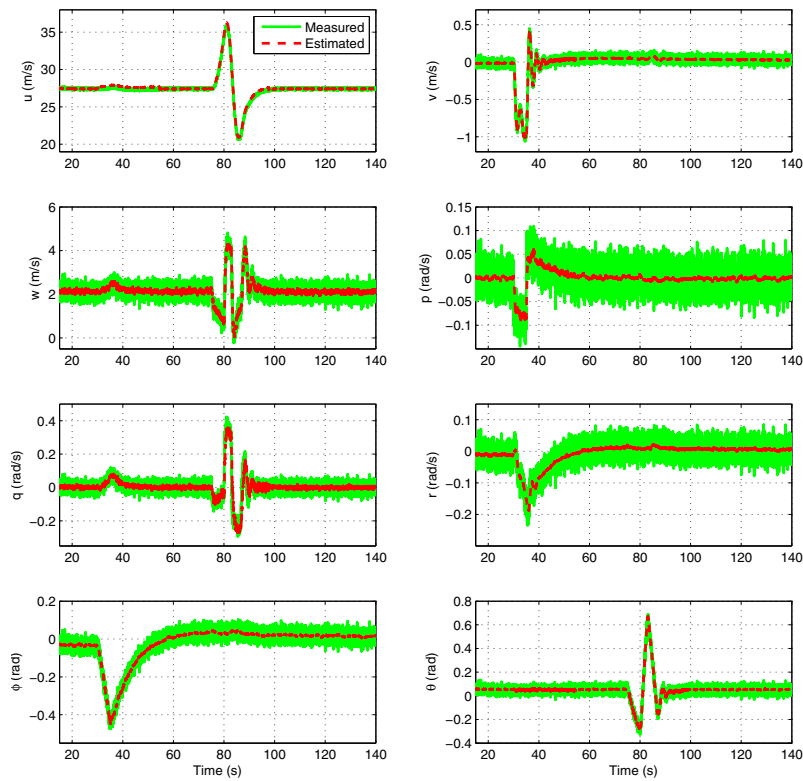
Fig. 7. Estimated states for LIP faults

Here, $\bar{x}(k)$ is the average value of the estimated actuator command. The mean squared error (MSE) σ aims to check the standard deviation of the estimate. γ is used to assess the estimation capacity when measurement noise is present.

For single floating actuator faults, 100 simulations are conducted with each lasting for $150s$ (simulation step is $0.01s$). The single faults occur within the time interval $[0, 150s]$ when the standard deviation of measurement noise increases. The estimate performance is illustrated in Fig. 8 and Fig. 9. For single aileron faults with magnitude variations between $[-7^o, 7^o]$, it is observed that the MSE is less than 1.05^o which indicates an accurate estimate of the faulty aileron. To quantify the acceptable estimate capacity, a threshold for the estimate capacity factor is required. The threshold is set to $-13.97\ dB$ in our case, which means the MSE is 20% of the maximum estimated aileron command. It is noticed in Fig. 8 that the estimate capacity factor γ remains less than the threshold until noise standard deviation is $0.16\ m/s$ in velocities, 0.13^o in attitudes and $0.13^o/s$ in angular rates. This indicates the FDD can tolerate measurement noise with standard deviations lower than these limit values. Similarly, single floating elevator fault is generated with increasing measurement noise to test estimate capacity of the FDD procedure. The elevator changes within $[-4^o, 4^o]$. It is shown in Fig. 9 that the MSE is less than 0.97^o for the estimated elevator. Also, the estimate capacity factor remains less than $-13.97\ dB$ until noise standard deviation reaches
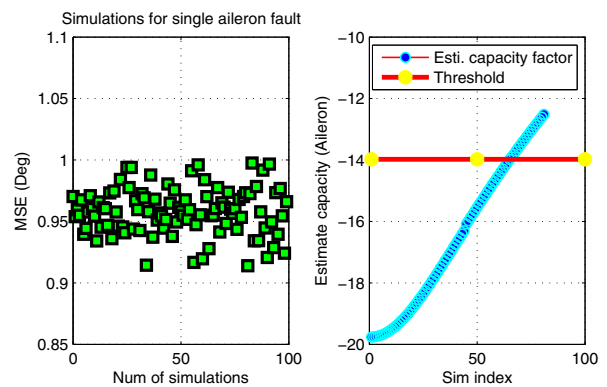
Fig. 8. MSE and estimate capacity factor for single floating aileron faults

$0.53\ m/s$ for velocities, 0.42^o for attitudes and $0.42^o/s$ for angular rates. It is seen that the proposed FDD procedure functions effectively when the measurement noise is within these limit values. Due to small measurement noise yielded by available sensors in the considered application, our FDD method can be applied to identification of single actuator faults.

6. CONCLUSION AND FUTURE WORK

In this paper, we present a recursive FDD scheme for identifying actuator faults with improved reliability. The fault detection is performed by using the UKF algorithm
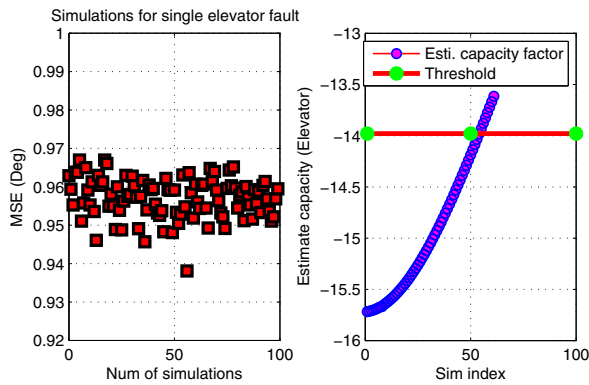
Fig. 9. MSE and estimate capacity factor for single floating elevator faults

and the fault diagnosis is conducted by the BC method. Performance of the proposed FDD is evaluated by using aerodynamic parameters of an ARCAA UAS and it is demonstrated in simulations that our method can effectively detect and isolate typical single actuator faults when measurement noise is present within certain levels. Future work includes assessment of our procedure for dual actuator fault scenarios (simultaneous occurrence of two actuator faults) and flight validation of the proposed FDD method. Also, performance of the proposed FDD framework will be tested for windy conditions.

REFERENCES

Amirarfaei, F., Baniamerian, A., and Khorasani, K. (2013). Joint kalman filtering and recursive maximum likelihood estimation approaches to fault detection and identification of boeing 747 sensors and actuators. In *AIAA Aerospace Science Meeting*.

Bernard, M., Kondak, K., Maza, I., and Ollero, A. (2011). Autonomous transportation and deployment with aerial robots for search and rescue missions. *Journal of Field Robotics*, 28, 914–931.

Brinker, J.S. and Wise, K.A. (2001). Flight testing of reconfigurable control law on the X-36 tailless aircraft. *Journal of Guidance, Control, and Dynamics*, 24, 903–909.

Calise, A.J., Lee, S., and Sharma, M. (2001). Development of a reconfigurable flight control law for tailless aircraft. *Journal of Guidance, Control, and Dynamics*, 24, 896–902.

Campbell, M.E. and Brunke, S. (2001). Nonlinear estimation of aircraft models for on-line control customization. In *IEEE Aerospace Conference*.

Ducard, G. and Geering, H.P. (2008). Efficient nonlinear actuator fault detection and isolation system for un-manned aerial vehicles. *Journal of Guidance, Control and Dynamics*, 31(1), 225–237.

Ducard, G.J.J. (2009). *Fault-tolerant Flight Control and Guidance Systems: Practical Methods for Small Unmanned Aerial Vehicles*. Springer, 1st edition.

Eide, F. and Maybeck, P. (1996). An MMAE failure detection system for the F-16. *IEEE Transactions on Aerospace and Electronics Systems*, 32, 1125–1136.

Julier, S.J. and Uhlmann, J.K. (2004). Unscented filtering and nonlinear estimation. In *Proc. of the IEEE*, volume 92, 401–422.

Kendoul, F. (2013). Towards a unified framework for uas autonomy and technology readiness assessment (atra). *Autonomous Control Systems and Vehicles*, 55–71.

Kim, S., Choi, J., and Kim, Y. (2008). Fault detection and diagnosis of aircraft actuators using fuzzy-tuning IMM filter. *IEEE Transactions on Aerospace and Electronic Systems*, 44, 940–952.

Lee, B.J., Park, J.B., Lee, H.J., and Joo, Y.H. (2005). Fuzzy-logic-based IMM algorithm for tracking a manoeuvring target. *IEE Proceedings on Radar Sonar Navigation*, 152, 16–22.

Maybeck, P.S. (1999). Multiple model adaptive algorithms for detecting and compensating sensor and actuator/surface failures in aircraft flight control systems. *International Journal of Robust and Nonlinear Control*, 9, 1051–1070.

Mejias, L. and Fitzgerald, D. (2013). A multi-layered approach for site detection in UAS emergency landing scenarios using geometry-based image segmentation. In *International Conference on Unmanned Aerial Systems*.

Mejias, L., Fitzgerald, D., Eng, P., and Liu, X. (2009). *Forced Landing Technologies for Unmanned Aerial Vehicles: Towards Safer Operations*, chapter Aerial Robotics, 415–442. InTech.

Meskin, N., Naderi, E., and Khorasani, K. (2013). A multiple model-based approach for fault diagnosis of jet engines. *IEEE Transactions on Control Systems Technology*, 21, 254–262.

Williams, P. and Crump, M. (2012). Intelligent landing system for landing uavs at unsurveyed airfields. In *28th International Congress of the Aeronautical Sciences*.

Yang, X., Mejias, L., and Molloy, T. (2013). Nonlinear $\mathcal{H}_\infty$ control of UAVs for collision avoidance in gusty environment. *Journal of Intelligent and Robotic Systems*, 69, 207–225.

Zhang, Y. and Jiang, J. (2000). Integrated design of reconfigurable fault-tolerant control systems. *Journal of Guidance*, 24, 133–136.

Zhang, Y. and Li, Z.R. (1998). Detection and diagnosis of sensor and actuator failures using IMM estimator. *IEEE Transactions on Aerospace and Electronic Systems*, 34(4), 1293–1313.